ZIBELINE INTERNATIONAL™ PUBLISHING

ISSN: 2222-7059 (Print)
EISSN: 2222-7067 (Online)

Advances in Industrial Engineering and Management (AIEM)

DOI: http://doi.org/10.7508/aiem.02.2024.91.105

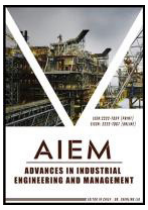

CrossMark

RESEARCH ARTICLE

SENSITIVITY ANALYSIS OF STABILITY PARAMETERS OF h-TYPE RETAINING STRUCTURE

Chuanxiang Xiong[a], Yuanyuan Xu[a,] Zhiquan Xing[b,c,*], Man Zhang[a], Zhiqiang Huang[d], Renjie Nie[b], Lei Zhu[b], Wentao Han[b], Wenjie Tang[a], David Hui[e], Yu Chen[b,c], Wei Chen[c,f,g,] En Lin[h], Shiyuan Sun[i], Shuping Lin[j], Huojin Su[k], Xiaoqun Lin[l], Yitao Chen[m]

[a] Zijin School of Geology and Mining, Fuzhou University, Fuzhou 350116, China
[b] College of Civil Engineering, Fuzhou University, Fuzhou 350116, China
[c] International and Hong Kong, Macao and Taiwan Joint Laboratory of Structural Engineering, Fuzhou University, Fuzhou 350116, China
[d] Fujian Academy of Building Research Co., Ltd., Fuzhou 350108, China
[e] Department of Mechanical Engineering, University of New Orleans, New Orleans, LA 70148, USA
[f] Chinese National Engineering Research Centre for Steel Construction (Hong Kong Branch), The Hong Kong Polytechnic University, Hong Kong SAR, China
[g] Department of Civil and Environmental Engineering, The Hong Kong Polytechnic University, Hong Kong SAR, China
[h] Fujian Rongsheng Construction and Development Co., Ltd. Fuzhou 350200, China
[i] Zhongqing Construction Group Co.,Ltd., Changchun 130000, China
[j] Fujian Yuxun Construction Co., Ltd., Zhangzhou 363107, China
[k] Fujian Wuzhou Construction Group Co., Ltd., Quanzhou 362400, China
[l] Fujian Jingsheng Municipal Garden Group Co., Ltd., Fuzhou 350000 china
[m] Hohai University,Nanjing, 210098, China

**Corresponding Author E-mail: 220525041@fzu.edu.cn*

ARTICLE DETAILS

Article History:

Received 30 October2023
Accepted 24 November 2023
Available online 29 December 2023

ABSTRACT

The stability of h-type anti-slide pile, a novel slope retaining structure, has received limited research attention in terms. In this study, we conducted a comparative analysis of indoor small-scale tests and established a numerical analysis model for actual engineering scenario. By employing the finite element strength reduction method, the effects of geometric and soil parameters on the stability of h-type anti-slide piles and the failure mode of the slope. The sensitivity factors affecting slope stability are studied by orthogonal analysis. Findings indicate that the sensitivity factors, ranked from high to low, are the internal friction angle (φ), cohesion (c), front and rear pile row distance (B/L_2), and front pile length (L_3/L_2). These four parameters exhibit a significant correlation with the sensitivity of the safety factor of slope stability. On this basis, the simplified formula for calculating the safety factor of slope stability is derived.

KEYWORDS

H-Type Retaining Structure, Slope Stability, Numerical Simulation, Strength Reduction Method, Sensitivity Analysis

1. INTRODUCTION

The h-type anti-slide pile is a novel slope retaining structure that has evolved from the portal double row pile supporting structure. It has been increasingly used in slope engineering (Akdag, 2016; Karalar and Dicleli, 2023; Kourkoulis et al., 2012; Liu et al., 2018; Wang et al., 2022; Xiong et al., 2022; Zhao et al., 2017). Currently, most studies have concentrated on analyzing the mechanical behavior and failure mode of anti-slide piles. However, there is a limited amount of research on the stability and sensitive factors of h-type retaining structure. Therefore, conducting research in this area holds significant importance.

Stability analysis is the foundation of slope engineering. The existing slope stability analysis methods mainly include limit balance method, limit analysis method, finite element method and so on. The limit equilibrium methods consist of the Swedish arc method, Bishop method, Janbu method, and others. In a study by Han et al. (2014), the influence of factors such as friction angle, slope angle, width to depth ratio, load and other factors on slope stability was investigated using the upper limit theorem of the limit analysis method. Xu and Yang (2018) examined the impact of slope angle, seismic force, soil heterogeneity and anisotropy on

Quick Response Code	Access this article online	
	Website: www.aiem.com.my	DOI: 10.7508/aiem.02.2024.91.105

Cite The Article: Chuanxiang Xiong, Yuanyuan Xu, Zhiquan Xing, Man Zhang, Zhiqiang Huang, Renjie Nie, Lei Zhu, Wentao Han, Wenjie Tang, David Hui, Yu Chen, Wei Chen, En Lin, Shiyuan Sun, Shuping Lin, Huojin Su, Xiaoqun Lin, Yitao Chen (2024). Sensitivity Analysis of Stability Parameters of h-Type Retaining Structure. *Advances In Industrial Engineering And Management*, 13(2): 91-105.

slope stability using the limit analysis method, and calculated the three-dimensional seismic and static stability of the slope. Zhang et al. (2017), based on the Bishop method, analyzed the effect of curvature radius and arch height on the stability of concave slopes and derived a formula for calculating the stability coefficient of concave slopes in cases of arc sliding. Deng et al. (2017) established a new limit equilibrium method based on the stress assumption based on the sliding surface to analyze the stability of the slope strengthened by micro anti-slide piles. In comparison to the limit equilibrium method, the finite element method offers a better consideration of the nonlinear constitutive relationship of rock and soil mass, and effectively captures the variations in safety factor at each stage of slope. As a result, the finite element method has gained widespread application (Won et al., 2005). Zhang et al. (2015) utilized the finite element method to study the influence of soil strength, geometric shape of foundation pit excavation and wall stiffness on slope stability. Similarly, Lim et al. (2017) employed the finite element limit analysis method to examine the stability and failure mechanism of slopes with different characteristics, such as soft soil slope, post-earthquake slope and rock slope. Rao et al. (2019) calculated the safety factor of slope stability through the finite element strength reduction method, and studied the influence of different soil heterogeneity and cohesion anisotropy on slope stability and anti-slide pile position. Lin et al. (2020) utilized the finite element strength reduction method to examine the influence of various reinforcement techniques, including anti-slide piles, anchor cables, and concrete support structures, on slope stability and reinforcement effectiveness. Since there are many factors affecting the stability of slope, sensitivity analysis can systematically evaluate the factors affecting the stability of slope (Castillo et al., 2008), and scientifically and reasonably evaluate the importance of each influencing factor to the test index, improve the analysis efficiency, and is widely used in the design of engineering structures. Therefore, scholars at home and abroad have done a lot of research on the sensitivity analysis of design parameters of slope stability. Sivakumar and Murthy (2005) conducted an analysis on the influence of design variables such as saturated hydraulic conductivity and suction parameters on slope stability in unsaturated soil. Ahour et al. (2020), using the generalized Hoek-Brown failure criterion, investigated the impact of additional load on the stability of rock slope through the finite element method. They also provided a sensitivity sequence for parameters such as slope angle, height, surcharge load intensity, and unconfined compressive strength of the rock. Raghuvanshi (2019) examined the influence of factors like slope angle, dip of potential failure plane, slope height, cohesion, and internal friction angle on slope stability using the one-way Analysis-of-Variance method, and presented the corresponding sensitivity sequence. Jiang et al. (2018) analyzed the sensitivity and influence of various slope design parameters, seismic load and physical and mechanical parameters of rock mass on slope stability under earthquake action. Chang et al. (2018) utilized the control variable method and orthogonal design method to investigate the sensitivity of factors such as internal friction angle and cohesion on slope stability under freeze-thaw failure. Lian and Wu (2021) employed the orthogonal experimental design method to analyze the sensitivity of geometric parameters, such as embedding depth and skeleton width, on the shallow stability of soil slopes reinforced by frame protective structures, and provided a sensitivity sequence for these parameters. Ghadrdan et al. (2020) conducted a study using the limit equilibrium method and finite element method to study the sensitivity of soil material properties such as internal friction angle, cohesion, permeability and creep to the stability of deep foundation pit in Australia. Zhou et al. (2020) analyzed the influence of geometric parameters such as step width, retaining wall length and excavation depth on the structural displacement of retaining wall based on the finite element method, and used the multiple adaptive regression spline method to analyze the sensitivity of supporting piles with different geometric parameters. Xu et al. (2021) established a slope stability analysis model by strength reduction method, taking into account the influencing factors such as elastic modulus of backfill soil, cohesion, internal friction angle and slope rate, and conducted sensitivity analysis on factors affecting the stability of subgrade slope through parameter study. Karthik et al. (2022) carried out finite element sensitivity analysis on the homogeneous slope containing soil with c-φ values, and evaluated the safety factor of the slope, considering the influence factors such as soil parameter and slope geometry.

The above research indicates that there are many factors affecting the stability and sensitivity of h-type slope retaining structure, and further research is needed. However, physical test has some limitations, it is difficult to fully reflect the influence of geometric characteristics, material characteristics, boundary characteristics of retaining structure on the stability of the actual engineering environment. In this paper, Optum G2, a numerical analysis software, was used to establish a numerical analysis model suitable for practical engineering based on a comparative analysis of small-scale indoor tests. The influence of geometric parameters and soil parameters on the stability of h-type anti-slide pile and the failure mode of slope was analyzed by strength reduction method of finite element. The sensitivity analysis of the influencing factors of slope stability and the simplified calculation formula of the safety factor of slope stability are derived can effectively evaluate the stability of slope and have a certain guiding effect on the theory and practical application of slope engineering.

2. ESTABLISHMENT OF NUMERICAL MODEL

2.1 Test basis of model establishment

In this paper, the small-scale test was simulated using Optum G2, a numerical analysis software. The finite element grid is depicted in Figure 1, where L_1 represents the length of the rear pile, L_2 is the length of the

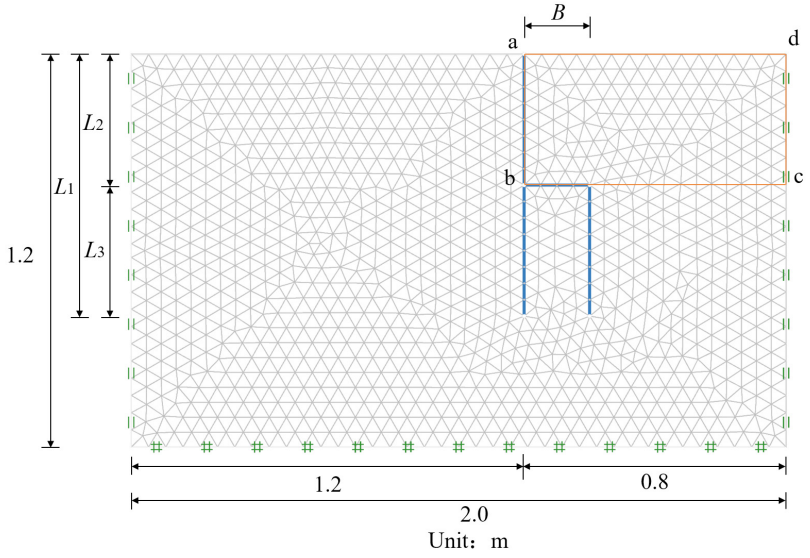

Figure 1: Finite element mesh diagram

cantilever section of the rear pile, L_3 denotes the length of the front pile, *S* represents the distance between the left and right adjacent piles, and *B* represents the row distance between the front and rear piles. The piles adopt a plate unit, and the reduction coefficient of the pile-soil contact surface is 0.7. The numerical model is used to simulate excavation under different conditions, which is consistent with the physical test in reference (Xiong et al., 2022). The excavation area is labeled as 'abcd', where only vertical displacement is allowed on the left and right edges, the bottom is a fixed constraint, and the top is a free boundary. The excavation units are deleted successively according to the working conditions. Stability is analyzed using the strength reduction method. Until the failure, the reduction multiple of c and φ values is the stability safety factor F_S of each group of slopes. The numerical analysis consists of 4000 units.

The selection of parameters. The hardened Mohr-Coulomb constitutive model is chosen as the soil constitutive model. The soil parameters adopted are consistent with those in literature (Xiong et al., 2022). The h-type retaining structure is equivalent to plate structure with corresponding thickness by using equivalent stiffness method. Soil parameters and pile parameters are shown in Table 1 and Table 2. This section mainly analyzes the pile bending moment and failure mode.

Pile bending moment is examined in Figure 2, the numerical calculation results of the bending moments of the measuring points under the excavation conditions of 0.1 m, 0.3 m and 0.45 m in each scheme are compared with the measured results. The distribution of bending moment and the influence of geometrical factors in the numerical simulation are basically consistent with the experiment.

The front pile body is located under the excavation face, and the bending moment shows little change at the beginning of excavation. Therefore, the bending moment value after excavation is selected for comparison.

Table 1: Soil parameters

Material	Modulus of compression E (MPa)	Poisson's ratio υ	Bulk density Γ (kN/m^3)	Cohesion C (kPa)	Angle of internal friction Φ (°)
Sandy soil	18	0.2	14	0	31

Table 2: The retaining structure parameters after equivalent

Parameter	Front and back pile	Connecting beam	Unit
Normal stiffness EA	1.183×10^4	7.554×10^5	kN/m
Flexural stiffness EI	0.1	25.31	kN·m^2/m
Yield force n_p	200	400	kN/m
Yield bending moment m_p	0.5	2	kN·m/m
Equivalent thickness t	10	20	mm

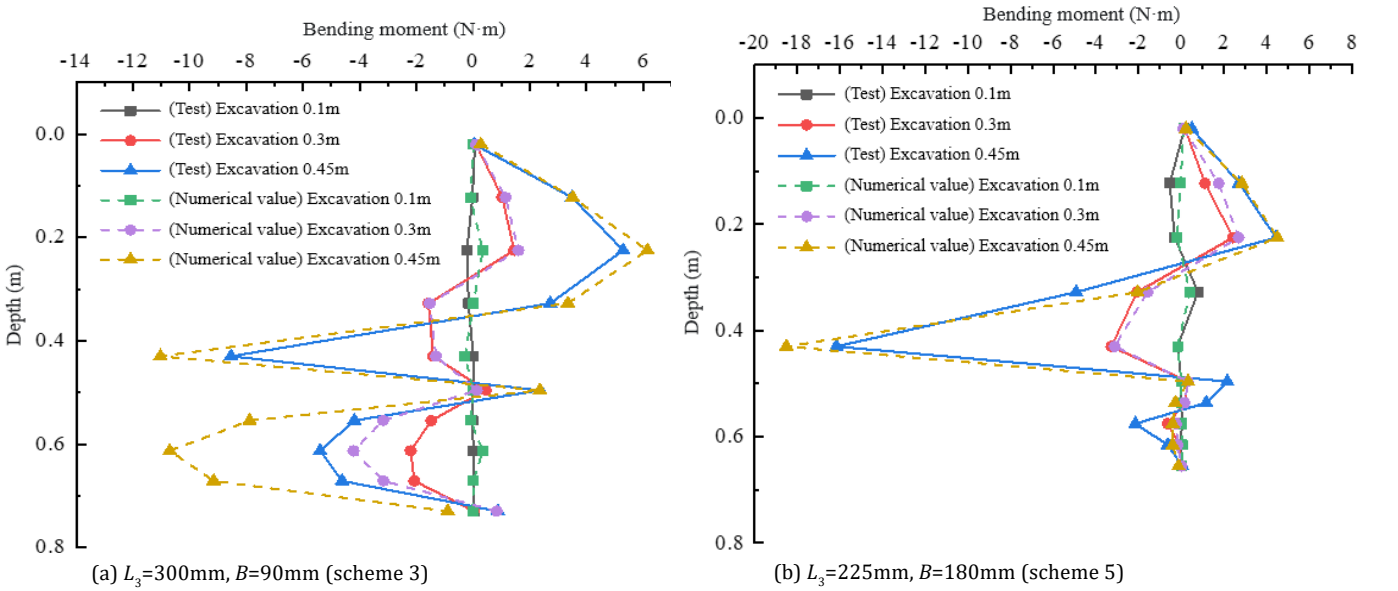

(a) L_3=300mm, B=90mm (scheme 3)

(b) L_3=225mm, B=180mm (scheme 5)

Figure 2: Comparison of bending moment of piles at the back row during excavation process

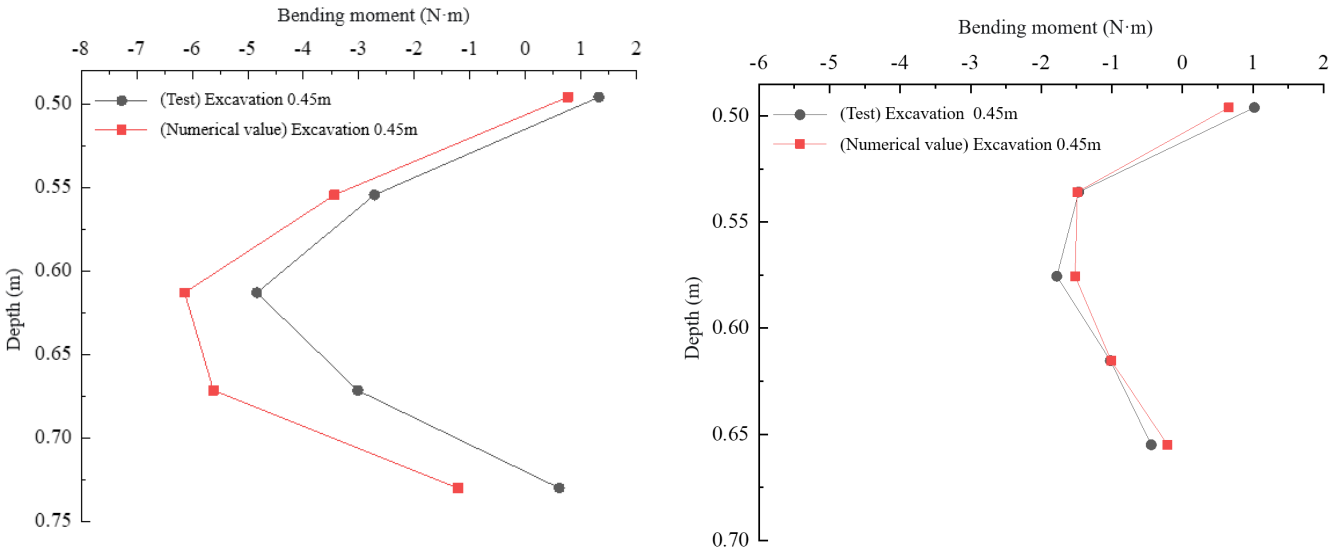

(a)L_3=300 mm, B=90 mm (scheme 3)

(b) L_3=225 mm, B=180 mm (scheme 5)

Figure 3: Comparison of bending moment of front row piles after excavation was completed

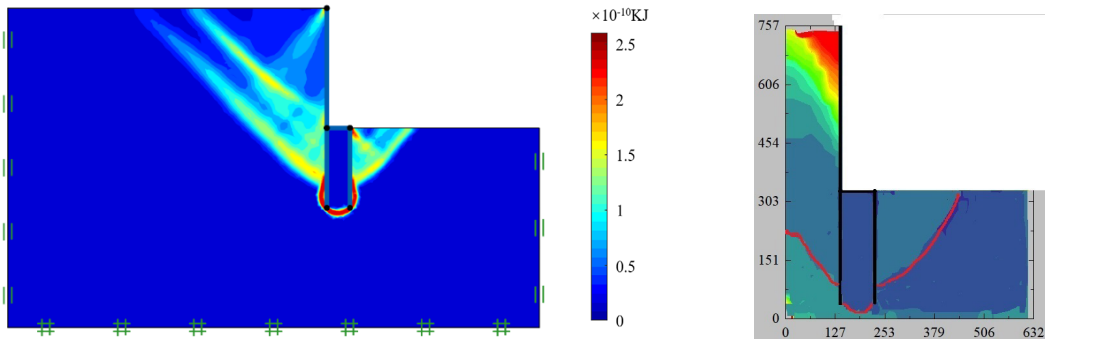

Shear dissipation diagram

Photoinfor deformation cloud diagram

(a) L_3=300 mm, B=90 mm(scheme 3)

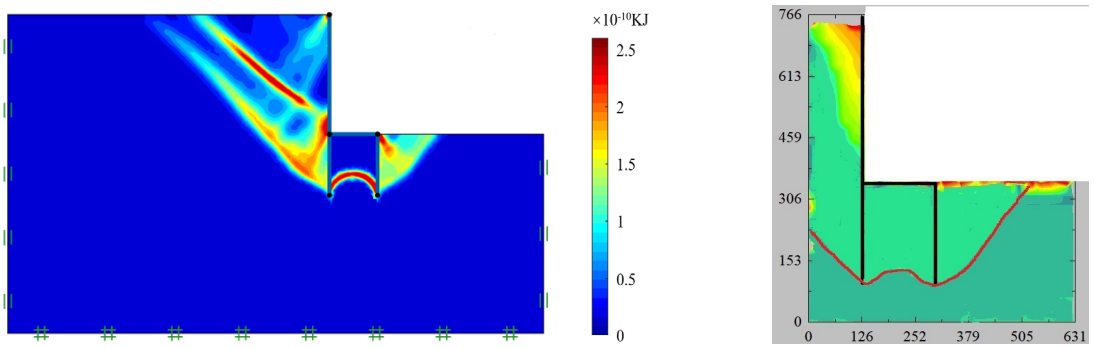

Shear dissipation diagram

Photoinfor deformation cloud diagram

(b)L_3=225 mm, B=180 mm(scheme 5)

Figure 4: Shear dissipation diagram and soil deformation cloud diagram

In Figure 3, the numerical calculation results of pile bending moments at each measuring point of the front pile in each scheme are compared with the measured data of the model test. It can be observed from the figure that the overall change trend of the two methods is consistent and relatively close.

Destruction mode. Figure 4 presents the shear dissipation diagram obtained from the numerical simulation after the completion of excavation, along with the soil deformation nephogram observed during the physical test. The soil deformation was recorded using the digital measurement software Photoinfor, which divided the grid points of the images throughout the entire excavation process of the physical test. The soil deformation cloud map was then generated by processing the PostViewer software. Both the test image analysis and numerical simulation clearly indicate the presence of two main types of sliding surfaces in slope failure under the support of the h-type retaining structure, namely the 'V' and 'W' surfaces, which are in agreement.

It is not difficult to see that the results of numerical analysis are close to those of physical test. The findings indicate that the geometric characteristics, material properties, and boundary processing methods employed in the numerical simulation process are rational. Furthermore,

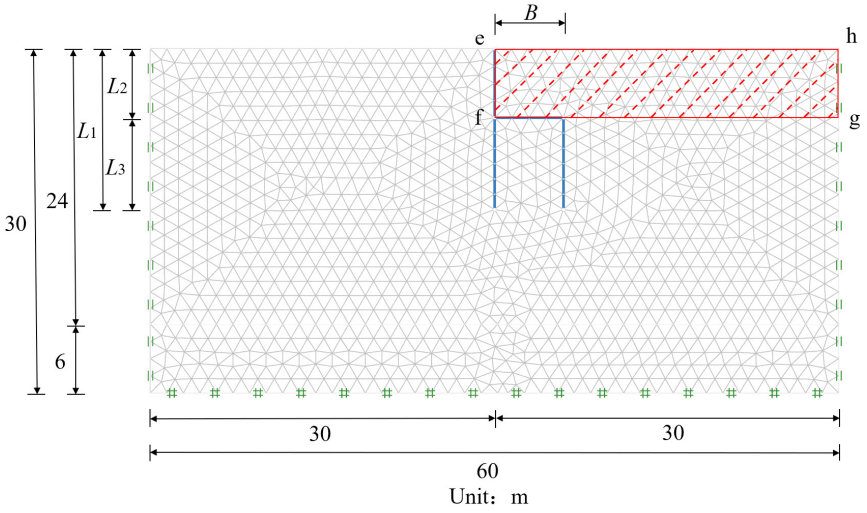

Figure 5: Finite element mesh diagram

the same methodology can be applied to assess the stability sensitivity of h-type retaining structures.

2.2 Establishment of the model

Model test can reveal the bearing mechanism and failure mechanism of retaining structure, but the cost of model test is expensive and it is difficult to exhaust all possible schemes. This paper uses the actual project and Chen and Yang (2005) to carry on the parameter analysis. The geotechnical layer within the influence range of the retaining structure consists of residual cohesive soil in the upper layer and strongly weathered granite in the lower layer. The soil parameters are provided in Table 3. Figure 5 depicts the finite element grid diagram, with 'efgh' representing the excavation area. The left and right edges allow only vertical displacement, while the bottom is fixed and the top is a free boundary. The retaining structure consists of manually dug and cast-in-place piles with a diameter of 900 mm and a distance of 2 m for both the front and back piles. The connecting beams are reinforced concrete beams measuring 800 mm×800 mm. By using the equivalent stiffness method, the front and rear piles, as well as the connecting beams, are considered equivalent to underground diaphragm walls with corresponding thickness. The material parameters of the supporting structure can be found in Table 4.

Table 3: Values of soil parameters

Parameter Soil layer	Layer thickness H (m)	Bulk density Γ (kN/m^3)	Modulus of compression E (MPa)	Cohesion C (kPa)	Angle of internal friction Φ (°)
Clay soil 24		17.6	4	18	15
Highly weathered granite	6	21.5	55	40	35

Table 4: Values of retaining structure parameters

Parameter	Front and back pile	Connecting beam	Unit
Normal stiffness EA	1.7×10^7	1.4×10^7	kN/m
Flexural stiffness EI	5×10^5	2.5×10^5	kN·m^2/m
Yield force n_p	5000	5000	kN/m
Yield bending moment m_p	800	800	kN·m/m

Table 5: Geometric parameter values of retaining structures			
Parameter	L_2 (m)	B/L_2	L_3/L_2
Value	6	0.2, 0.4, 0.6, 0.8, 1.0, 1.2	0.5, 1.0, 1.5, 2.0, 2.5

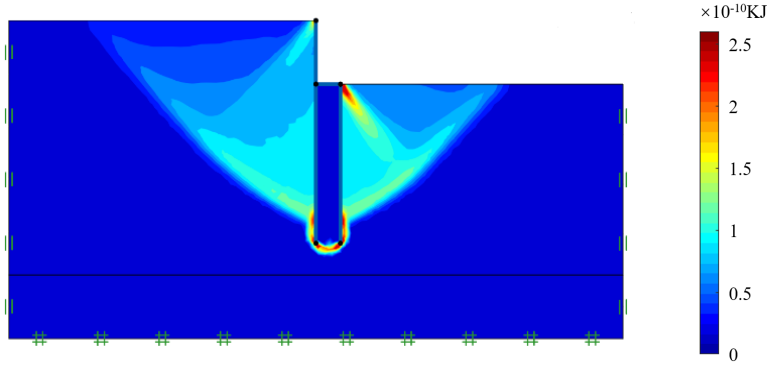

(a) B/L_2=0.4

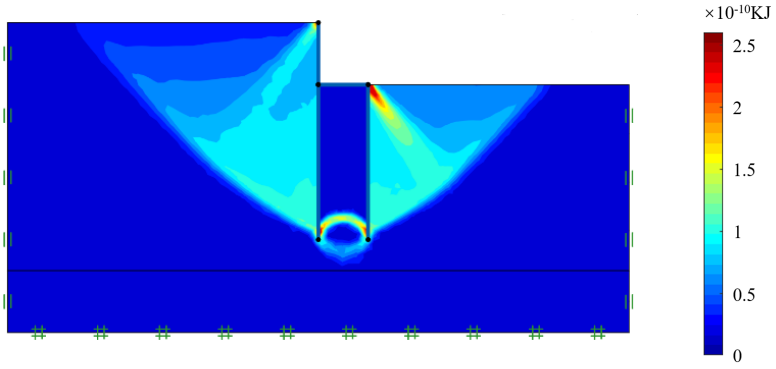

(b) B/L_2=0.8

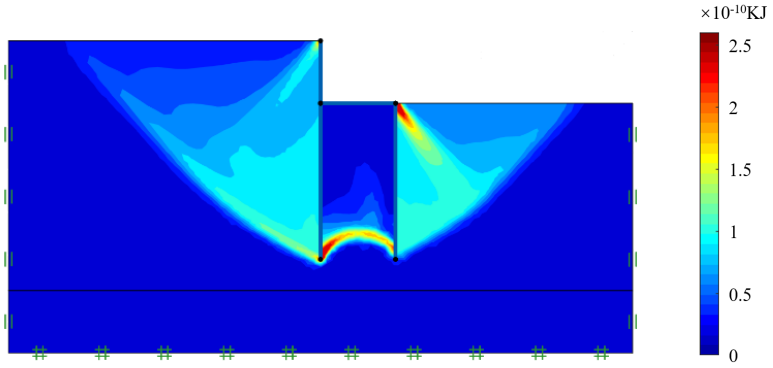

(c) B/L_2=1.2

Figure 6: Shear dissipation diagram under different pile row spacing B

3. FAILURE MODE AND STABILITY ANALYSIS

3.1 Influence of geometric parameters

The geometric characteristics of a retaining structure refer to the length of the front and back piles as well as the distance between them. To facilitate the analysis, the geometric features were processed dimensionlessly. The parameters B/L_2 and L_3/L_2 were selected for analysis, where B represents the row distance between the front and rear piles, L_3 is the length of the front pile, and L_2 is the length of the cantilever section of the rear pile. The parameter values are presented in Table 5.

3.1.1 Influence of front and rear pile row spacing

The study adopted the control variable method, with L_3/L_2=2.5 and L_2=6 m kept unchanged. B/L_2 was set as variables 0.2, 0.4, 0.6, 0.8, 1.0 and 1.2 for simulation analysis.

As shown in Figure 6(a), when B/L_2 is very small, the sliding surface on both sides, intersects with the pile body at the upper part of the pile bottom and forms a circular sliding surface under the pile, forming a 'V' shape as a whole. Because the width of soil between piles is too small, the performance of retaining structure tends to be similar to that of single row pile. Therefore, the front and rear piles overturn around the pile bottom as a whole, and the failure mode is V-shaped. With the increase of B, the soil behind the pile initially undergoes plastic flow, followed by the soil between the piles. This plastic flow gradually expands, eventually forming a sliding surface, as depicted in Figure 6(b).

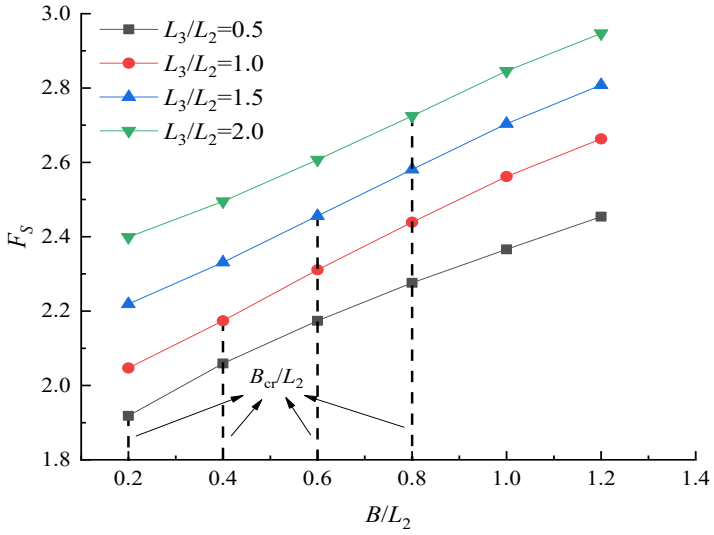

Figure 7: Stability safety factor under different front and rear pile row spacing *B*

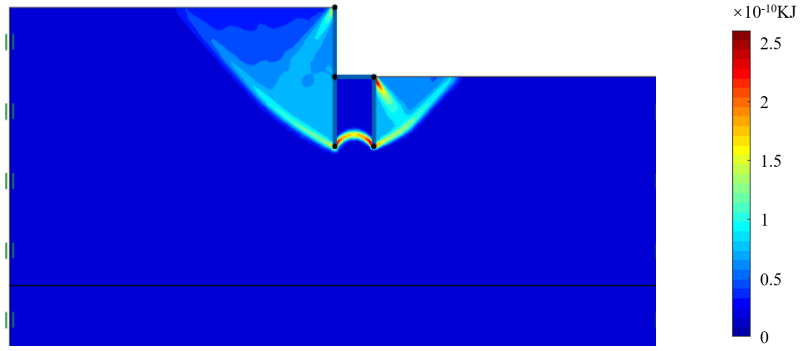

(a) L_3/L_2=1.0

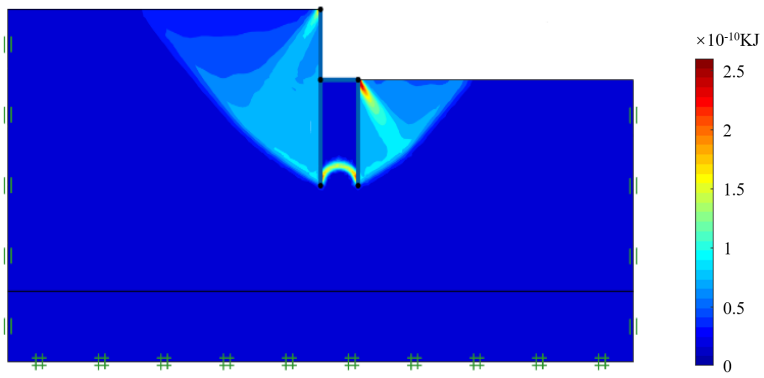

(b) L_3/L_2=1.5

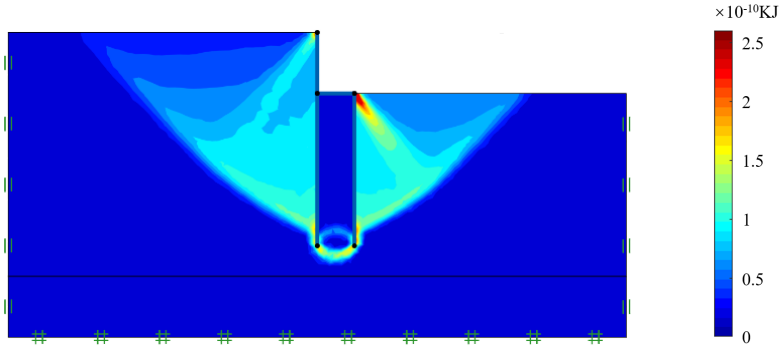

(c) L_3/L_2=2.5

Figure 8: Shear dissipation diagram under different front pile lengths L_3

Cite The Article: Chuanxiang Xiong, Yuanyuan Xu, Zhiquan Xing, Man Zhang, Zhiqiang Huang, Renjie Nie, Lei Zhu, Wentao Han, Wenjie Tang, David Hui, Yu Chen, Wei Chen, En Lin, Shiyuan Sun, Shuping Lin, Huojin Su, Xiaoqun Lin, Yitao Chen (2024). Sensitivity Analysis of Stability Parameters of h-Type Retaining Structure. *Advances In Industrial Engineering And Management*, 13(2): 91-105.

Figure 6(c) shows the shear strain of the slope when B/L_2 is large. When B increases to a certain extent, the shear plane of the left supporting zone completely reaches the pile bottom, and the soil behind the pile only flows plastic to the pile, and an arc-shaped shear zone with obvious internal convex is generated, showing the overall shape of 'W'. At this time, the interaction of front pile, soil between piles and back pile is strengthened, especially the reaction of pile bottom. The damage mode is 'W'.

Figure 7 illustrates the variation of the safety factor F_S of slope stability with the distance between the front and rear piles when L_3/L_2 values are 0.5, 1.0, 1.5, and 2.0. With the increase of B/L_2, the safety factor F_S of slope stability increases gradually. In order to guide the engineering practice to judge the failure mode, the critical distance between front and rear pile rows B_{cr} is introduced; When $B/L_2 < B_{cr}/L_2$, the slope failure mode is 'V' font; otherwise, the slope failure mode is 'W' font.

3.1.2 Influence of front pile length

When studying the influence of front pile length (L_3) on the failure mode and stability safety factor of the slope supported by an h-type retaining structure, B/L_2=0.6 and L_2=6 m remain unchanged. The value of L_3/L_2 can be 0.5, 1.0, 1.5, 2.0, or 2.5.

As shown in Figure 8(a), when the current pile length is relatively small, the shear planes on both sides intersect with the back pile and the front pile respectively at the bottom of the pile, and an obvious through-circular shear zone is formed between the piles. At this time, the failure mode of 'W' is presented (Figure 8(a)). As the length of the front pile increases, the plastic flow of soil between the piles weakens and the range of shear on both sides expands outward. This indicates that increasing the length of the front pile contributes to enhancing the slope stability (Figure 8(b)). When the front pile length increases to a certain extent, as depicted in Figure 8(c), the shear plane of soil on both sides of the pile is blocked above the pile bottom by the front and back piles, which significantly reduces the plastic flow through the pile bottom to the pile, leading to the weakening of the pile bottom reaction and the overall overturning failure along the pile bottom in an arc shape. In this scenario, the failure mode is V-shaped, as shown in Figure 8(b). Simultaneously, the influence range of the failure surface is further expanded, thereby enhancing the slope stability.

Figure 9 shows the curve of slope stability safety factor (F_S) of L_3 with different front pile lengths varying with front pile lengths. The value of B/L_2 is 0.2, 0.4, 0.6, and 0.8. It observed that as the length of the front pile increases, the stability safety factor tends to increase. In order to facilitate the guidance of practice, the critical front pile length $(L_3)_{cr}$ is introduced, that is, under the condition that B/L_2 is not less than B_{cr}/L_2, when L_3/L_2 is not more than $(L_3)_{cr}/L_2$, the slope failure mode is 'W' shape. Conversely, the slope failure mode is 'V' shape.

3.2 Influence analysis of soil parameters

Cohesion (c) and internal friction angle (φ) are strength indexes of soil. These parameters have a significant impact on the failure mode and stability safety factor of a slope, under the same geometric parameters. Table 6 provides the geometric parameters and soil parameters.

3.2.1 Influence of cohesion

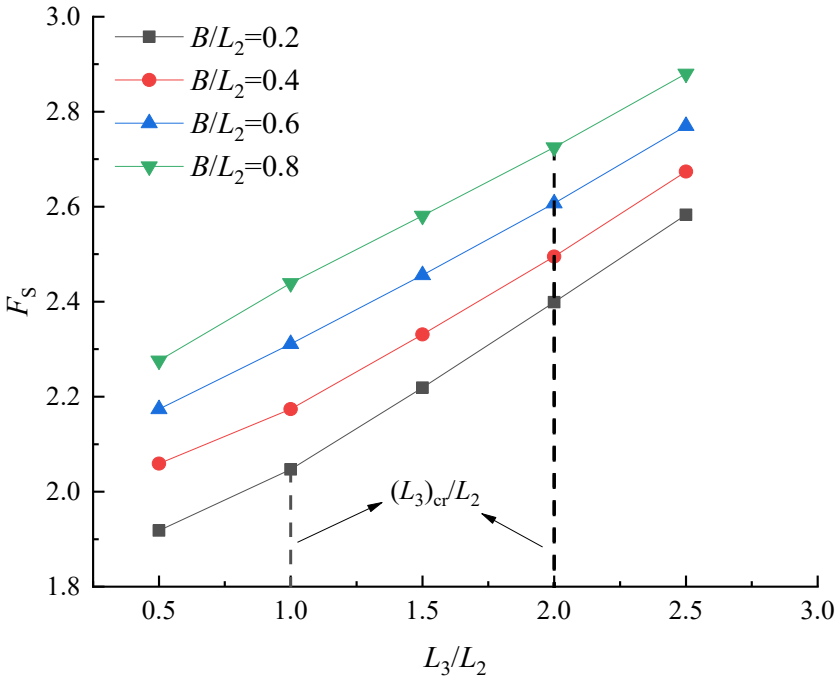

Figure 9: Stability safety factor under different front pile lengths L_3

Table 6: Geometrical parameters and soil parameters

Parameter	B/L_2	L_3/L_2	c (kPa)	φ (°)
Value	1.00	1.25	18, 28, 38, 48, 58	15, 25, 35, 45, 55

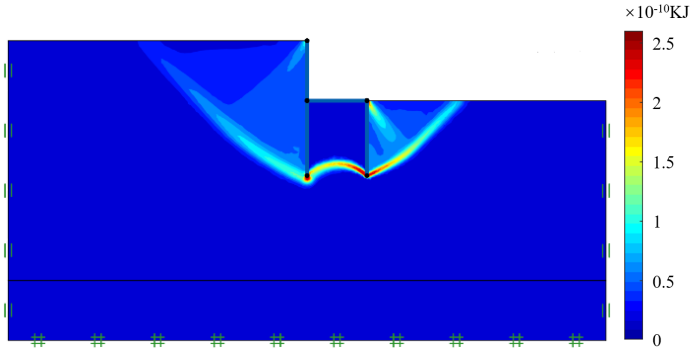

(a) c=18kPa

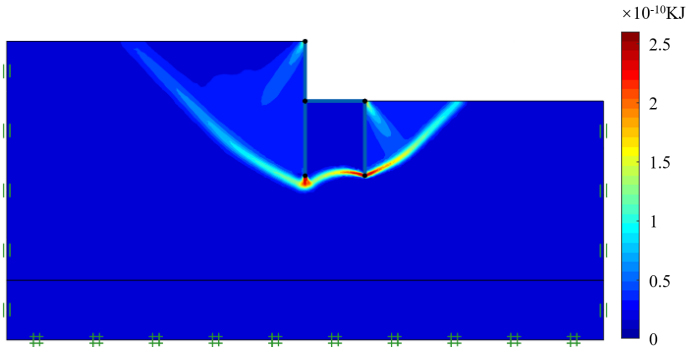

(b) c=38kPa

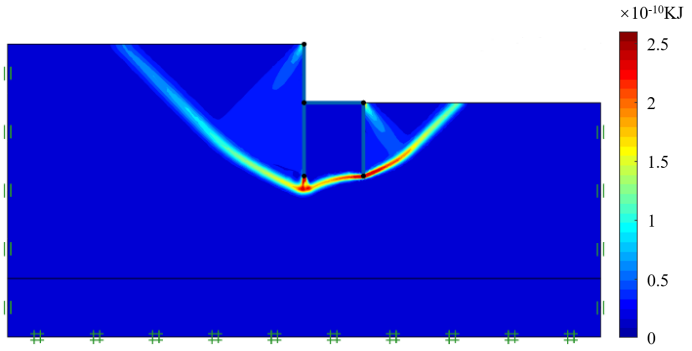

(c) c=58kPa

Figure 10: Shear dissipation diagram under different cohesive forces c

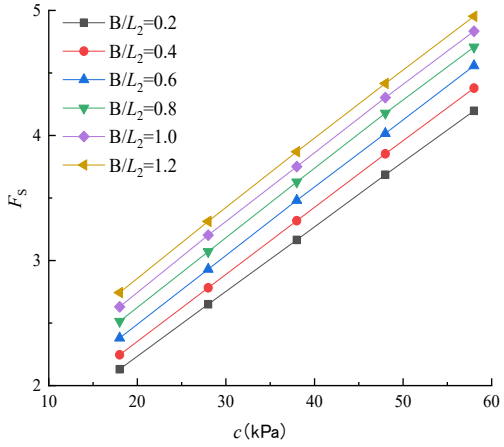

Figure 11: Stability safety factor under different cohesion c

When B/L_2=1.00, L_3/L_2=1.25 and φ=15° remain unchanged, the influence of different cohesion (c) on the failure mode and stability safety factor of slope supported by an h-type retaining structure is studied. Figure 10 displays the shear dissipation diagram obtained through strength reduction analysis for varying cohesion.

By comparing Figs. 10(a)-(c), it can be observed that as cohesion, the intersection point between the left shear plane and the back pile gradually moves downward, and the slip plane between piles gradually becomes gentle. At the same time, the scope of failure surface on both sides increases to some extent. However, the overall failure pattern remains unchanged, indicating that increasing the cohesive force of the clay layer does not alter the failure pattern. With the increase of cohesion, the density of plastic flow on the shear plane on both sides also decreases, indicating that the increase of cohesion reduces the plastic flow along the sliding plane to some extent.

Figure 11 shows the variation of slope stability safety factor (F_S) with cohesion under different pile row spacing. As the cohesion increases, the safety factor of slope stability gradually improves, resulting in enhanced slope stability.

3.2.2 Influence of internal friction angle

When B/L_2=1.00, L_3/L_2=1.25 and c=18kPa are constant, the influence of internal friction angle (φ) on the failure mode and stability safety factor of the slope supported by h-type retaining structure is studied. Shear dissipation graphs corresponding to different internal friction angles are obtained through strength reduction analysis, as illustrated in Figure 12.

The analysis of Figure 12 shows that the change of internal friction angle almost does not change the type of slope failure mode. At the same time, the increase of internal friction angle can not only reduce the plastic flow of soil sliding surface, but also make more soil between piles participate in the resistance to lateral earth pressure.

Figure 13 shows the curve of slope stability safety factor changing with internal friction angle under different pile row spacing. It can be found that the increase of internal friction angle can obviously improve the safety factor of slope. This is because the increase of the internal friction angle not only reduces the plastic flow of soil, but also improves the anti-lateral movement ability of soil between piles, so that the stability of slope is obviously improved.

4. SENSITIVITY ANALYSIS OF INFLUENCING FACTORS

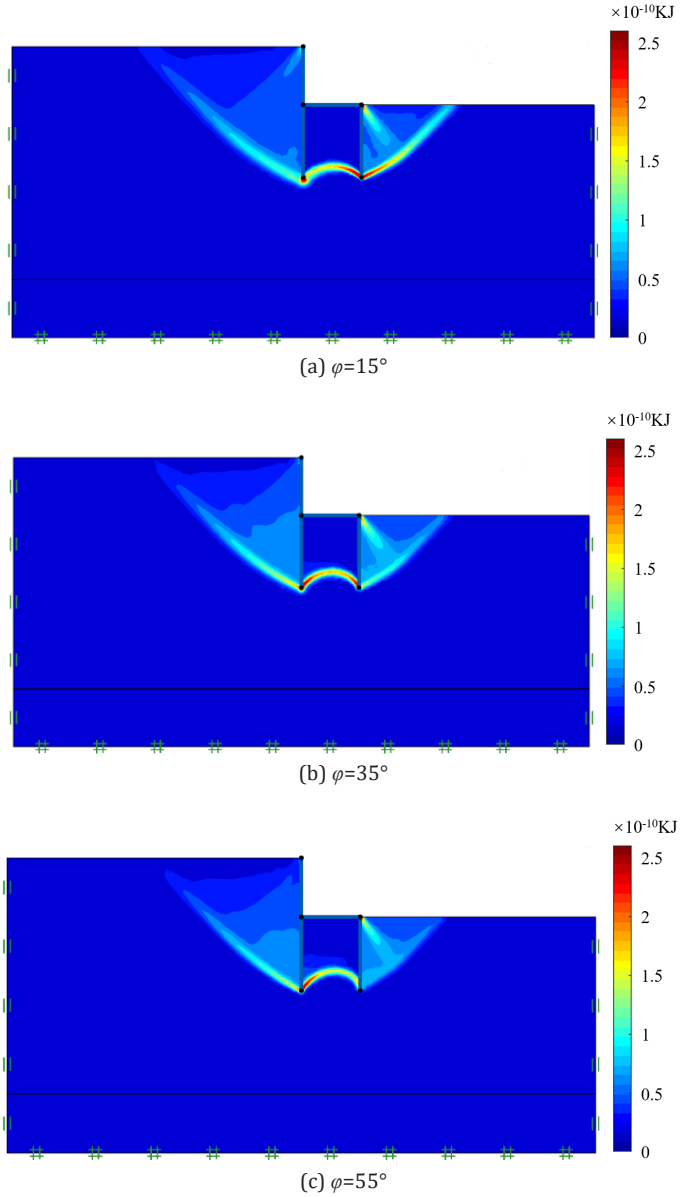

Figure 12: Shear dissipation diagram under different internal friction angles φ

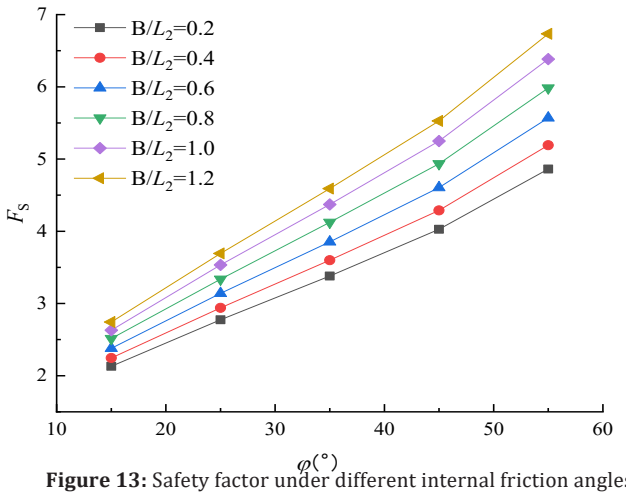

Figure 13: Safety factor under different internal friction angles φ

Table 7: Parameters and levels

Parameter	Level			
	1	2	3	4
L_3/L_2	0.5	1.0	1.5	2.0
B/L_2	0.4	0.6	0.8	1.0
c (kPa)	18	28	38	48
φ (°)	15	25	35	45

Table 8: Orthogonal experimental test scheme

Parameter	L_3/L_2	B/L_2	c (kPa)	φ (°)	Empty train	F_s
Test 1	0.5	0.4	18	15	1	2.059
Test 2	0.5	0.6	28	25	2	3.377
Test 3	0.5	0.8	38	35	3	4.79
Test 4	0.5	1	48	45	4	6.326
Test 5	1	0.4	28	35	4	3.981
Test 6	1	0.6	18	45	3	4.383
Test 7	1	0.8	48	15	2	4.115
Test 8	1	1	38	25	1	4.566
Test 9	1.5	0.4	38	45	2	5.632
Test 10	1.5	0.6	18	35	1	4.029
Test 11	1.5	0.8	48	25	4	5.130
Test 12	1.5	1	28	15	3	3.264
Test 13	2	0.4	48	25	3	4.927
Test 14	2	0.6	38	15	4	3.664
Test 15	2	0.8	25	45	1	6.152
Test 16	2	1	18	35	2	4.860

Sensitivity analysis of influencing factors aims to examine the correlation between factors that affect variables and the corresponding variables. This is measured by the ratio of the relative rate of change of each parameter to the relative rate of change between the study variables. The safety factor of slope stability can be influenced by different combinations of the four factors: front pile length, front pile row distance, cohesion, and internal friction angle. If the comprehensive test method is adopted, 4^4=256 tests need to be carried out according to the 4 factors and 4 levels of this test, and the workload is too large to achieve. The sensitivity degree of four factors to safety factor of slope

Table 9: Average value of test results at different levels for each parameters

Level	L_3/L_2	B/L_2	c	φ
1	4.138	4.150	3.833	3.276
2	4.261	3.863	4.194	4.500
3	4.514	5.047	4.663	4.415
4	4.901	4.754	5.125	5.623
Delta	0.763	1.184	1.292	2.347
Delta	4	3	2	1

Table 10: Analysis of Variance

Source of variance	Degree of freedom	Adj SS	Adj MS	F value	Test P value
L_3/L_2	3	1.362	0.454	14.227	0.028
B/L_2	3	1.098	0.366	11.493	0.038
c	3	2.181	0.727	22.797	0.014
φ	3	11.46	3.82	119.841	0.001
Error	3	0.096	0.032	-	-
Total	15	16.197	-	-	-

stability is analyzed by orthogonal test (Yan et al., 2023). Table 7 shows that the four parameters selected were L_3/L_2, B/L_2, c, and φ, with four levels set for each parameter. According to Table 8, table L_{16} (4^5) was used to arrange the test scheme, totaling 16 tests.

Table 9 and Table 10 present the mean value and variance analysis results for different levels of orthogonal test parameters. Delta represents the extreme value, with a higher value indicating a greater parameter influence. Adj SS refers to the sum of squares of the deviation mean, which is the sum of squares of the difference between each data point in the variable and the mean of the variable. Adj MS represents the mean square, calculated by dividing the corresponding Adj SS by the degree of freedom. F is the statistic used for hypothesis testing in analysis of variance, while P represents the probability of significance. From the analysis of the orthogonal test results, the sensitivity order of the four parameters to the safety factor of slope stability can be determined. The order, from high to low, is as follows: φ, c, B/L_2, L_3/L_2. The sensitivity of these four parameters to the safety factor of slope

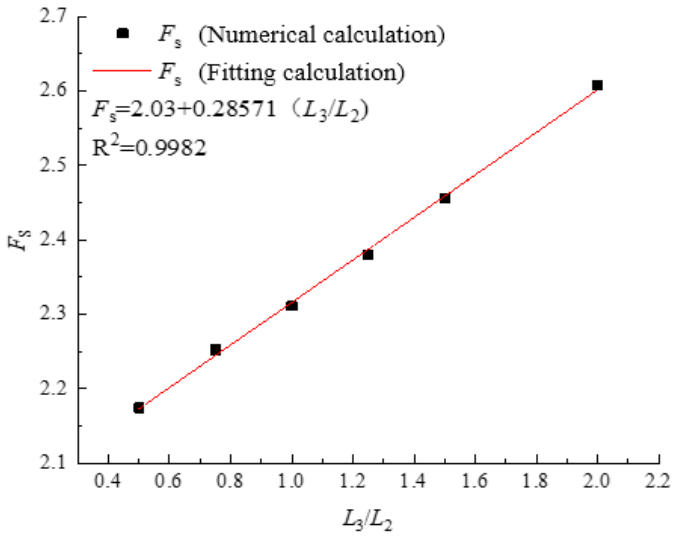

Figure 14: Fitting of relation between front pile length and safety factor

stability is significant. Therefore, if conditions permit, the soil can be improved to improve the strength of the soil, and then the geometric design of the pile can be optimized.

5. SIMPLIFIED CALCULATION OF STABILITY SAFETY FACTOR

The relationship between the safety factor of slope stability and the four parameters was established using regression analysis fitting method. This allowed for the derivation of a simplified formula for calculating the safety factor, making it more convenient to evaluate slope stability.

As shown in Figure 14, working conditions B/L_2=0.6, c=18kPa, and φ=15° are selected to carry out regression fitting of the relationship between the safety factor of slope stability andL_3/L_2, so that the relationship can be obtained:

$$F_s = 2.03 + 0.28571\frac{L_3}{L_2} \tag{1}$$

Based on Formula (1), the safety factor of slope stability is influenced by different pile row spacing, cohesion, and internal friction angle. To represent the influence of pile row spacing, cohesion, and internal friction angle on the safety factor of slope stability, three parameters f_B, f_c, and f_φ are introduced successively. The simplified calculation formula for the safety factor of slope stability under the support of an h-type retaining structure can be obtained as follows:

$$F_s = \left(2.03 + 0.28571\frac{L_3}{L_2}\right) f_B f_c f_\varphi \tag{2}$$

Similarly, the calculation formulas of f_B, f_c and f_φ can be obtained by regression fitting method as follows:

$$f_B = 0.84 + 2.6038\frac{B}{L_2} \tag{3}$$

$$f_c = 0.59 + 0.02288c \tag{4}$$

$$f_\varphi = 0.49 + 0.03289\varphi \tag{5}$$

As shown in Figure 15, the numerical calculation results and simplified formula calculation results of the safety factor of slope stability under the influence of four parameters (front pile length, front pile row distance, cohesion, and internal friction angle) are compared. Overall analysis reveals that the calculation result of the simplified formula is close to that of the numerical calculation. However, the simplified formula tends to yield slightly smaller overall calculation results, which is beneficial for enhancing project safety. Therefore, to some extent, the formula can be utilized for accurately evaluating slope stability.

6. CONCLUSION

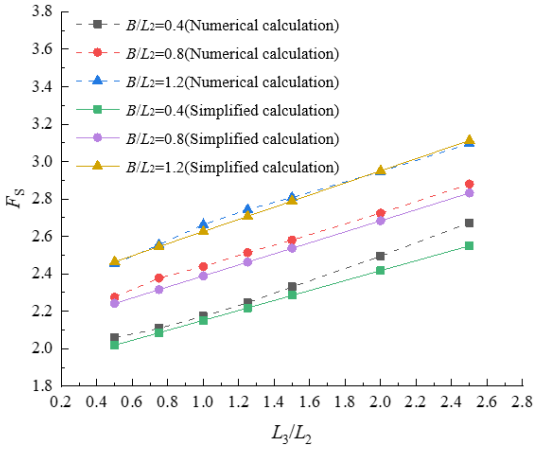

(a) Different front pile length

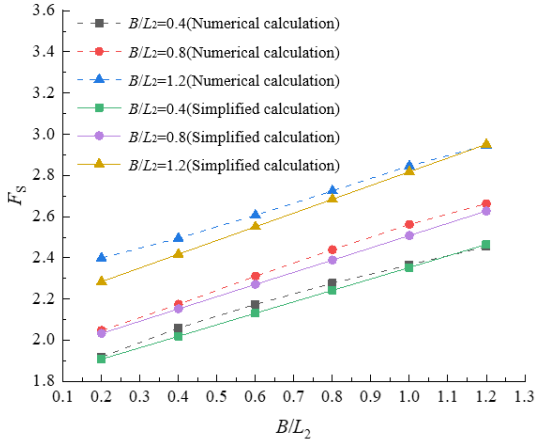

(b) Different pile spacing before and after

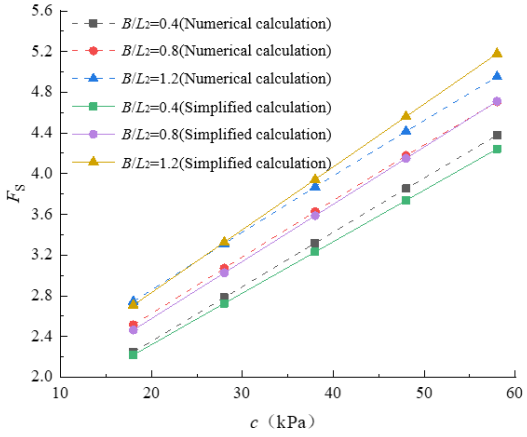

(c) Different cohesion

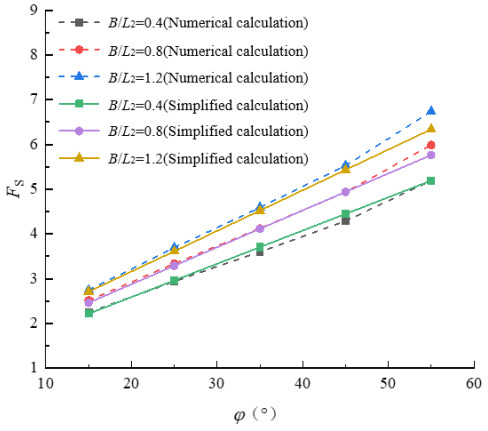

(d) Different angles of internal friction

Figure 15: Comparison between numerical calculation and simplified formula

Cite The Article: Chuanxiang Xiong, Yuanyuan Xu, Zhiquan Xing, Man Zhang, Zhiqiang Huang, Renjie Nie, Lei Zhu, Wentao Han, Wenjie Tang, David Hui, Yu Chen, Wei Chen, En Lin, Shiyuan Sun, Shuping Lin, Huojin Su, Xiaoqun Lin, Yitao Chen (2024). Sensitivity Analysis of Stability Parameters of h-Type Retaining Structure. *Advances In Industrial Engineering And Management*, 13(2): 91-105.

Through the verification of the physical model, the finite element model is established based on the actual project, and the influence of geometric parameters and soil parameters on the failure mode and stability safety factor of the slope is studied by strength reduction method. Through orthogonal analysis method, sensitivity analysis is carried out on the influencing factors of safety factor of slope stability, and through regression analysis method, simplified calculation formula of safety factor of slope stability is given, the main conclusions are as follows:

The bending moment and failure mode results of the numerical model align with those of the physical model test, thereby providing a reliable tool for the calculation and analysis of h-type retaining structure.

The distance between the front and rear pile rows is the most important factor affecting the failure mode of a slope. There are two failure modes depending on B_{cr}/L_2: when $B/L_2 < B_{cr}/L_2$, the failure mode of the slope is V-shaped. On the contrary, the failure mode of the slope is W-shaped. When the front pile row distance is large ($B/L_2 \geq B_{cr}/L_2$), and the front pile length is increased to $L_3/L_2 > (L_3)_{cr}/L_2$, the slope failure mode develops from 'W' shape to 'V' shape.

The increase of front and rear pile row distance, front pile length, internal friction angle and cohesion will significantly improve the safety factor of slope stability. The sensitivity of factors affecting the safety factor of slope stability follows this order: internal friction angle, cohesion, front and rear pile row distance, and front pile length. Therefore, to enhance slope stability, it is important to prioritize the strength of the soil and then optimize the geometric design of the pile.

The simplified formula of safety factor of slope stability based on regression analysis can be established to effectively evaluate the stability of slope.

The research on the design theory and method of slope retaining structure is of certain significance to practical engineering.

ACKNOWLEDGEMENTS

This research work was supported by Fifth Batch of Science and Technology Plan Project of Housing and Urban-Rural Construction Industry of Fujian Province in 2022 (No. 2022-K-297).

REFERENCES

Ahour, M., Hataf, N., Azar, E., 2020. A mathematical model based on artificial neural networks to predict the stability of rock slopes using the generalized Hoek–Brown failure criterion. Geotechnical and Geological Engineering, 38: Pp. 587-604.

Akdag, C.T., 2016. Behavior of closely spaced double-pile-supported jacket foundations for offshore wind energy converters. Applied Ocean Research, 58: Pp. 164-177.

Castillo, E., Mínguez, R., Castillo, C., 2008. Sensitivity analysis in optimization and reliability problems. Reliability Engineering & System Safety, 93(12): Pp. 788-1800.

Chang, Z.G., Cai, Q.X., Ma, L., Han, L., 2018. Sensitivity analysis of factors affecting time-dependent slope stability under freeze-thaw cycles. Mathematical Problems in Engineering, 2018: Pp. 7431465.

Chen, F.Q., Yang, M., 2005. Numerical analysis of piles influenced by lateral soil movement due to surcharge loads. Chinese Journal of Geotechnical Engineering, 27(11): Pp. 51-55.

Deng, D.P., Li, L., Zhao, L.H., 2017. Limit-equilibrium method for reinforced slope stability and optimum design of antislide micropile parameters. International Journal of Geomechanics, 17(2): Pp. 06016019.

Ghadrdan, M., Shaghaghi, T., Tolooiyan, A., 2020. Sensitivity of the stability assessment of a deep excavation to the material characterisations and analysis methods. Geomechanics and Geophysics for Geo-Energy and Geo-Resources, 6: Pp. 1-14.

Han, C.Y., Chen, J.J., Xia, X.H., Wang, J.H., 2014. Three-dimensional stability analysis of anisotropic and non-homogeneous slopes using limit analysis. Journal of Central South University, 21(3): Pp. 1142-1147.

Jiang, X.L., Niu, J.Y., Yang, H., Wang, F.F., 2018. Upper bound limit analysis for seismic stability of rock slope with tunnel. Advances in Civil Engineering, 2018: Pp. 1-11.

Karalar, M., Dicleli, M., 2023. Effect of pile orientation on the fatigue performance of jointless bridge H-piles subjected to cyclic flexural strains. Engineering Structures, 276: Pp. 115385.

Karthik, A.V.R., Manideep, R., Chavda, J.T., 2022. Sensitivity analysis of slope stability using finite element method. Innovative Infrastructure Solutions, 7(2): Pp. 184.

Kourkoulis, R., Gelagoti, F., Anastasopoulos, I., Gazetas, G., 2012. Hybrid method for analysis and design of slope stabilizing piles. Journal of Geotechnical and Geoenvironmental Engineering, 138(1): Pp. 1-14.

Lian, J.F., Wu, J.J., 2021. Shallow stability and parameter sensitivity analysis of soil slope with frame protection under rainfall seepage. Scientific Reports, 11(1): Pp. 19607.

Lim, K., Li, A.J., Schmid, A., Lyamin, A.V., 2017. Slope-stability assessments using finite-element limit-analysis methods. International Journal of Geomechanics, 17(2): Pp. 06016017.

Lin, C.N., Li, T.C., Zhao, L.H., Zhang, Z., Lin, C., Liu, X.Q., Niu, Z.W., 2020. Reinforcement effects and safety monitoring index for high steep slopes: A case study in China. Engineering Geology, 279:105861.

Liu, X.R., Kou, M.M., Feng, H., Zhou, Y., 2018. Experimental and numerical studies on the deformation response and retaining mechanism of h-type anti-sliding piles in clay landslide. Environmental earth sciences, 77: Pp. 1-14.

Raghuvanshi, T.K., 2019. Governing factors influence on rock slope stability–Statistical analysis for plane mode of failure. Journal of King Saud University-Science, 31(4): Pp. 1254-1263.

Rao, P.P., Zhao, L.X., Chen, Q.S., Nimbalkar, S., 2019. Three-dimensional limit analysis of slopes reinforced with piles in soils exhibiting heterogeneity and anisotropy in cohesion. Soil Dynamics and Earthquake Engineering, 121: Pp. 194-199.

Sivakumar, B.G.L., Murthy, D.S., 2005. Reliability analysis of unsaturated soil slopes. Journal of geotechnical and geoenvironmental engineering, 131(11): Pp. 1423-1428.

Wang, G., Dong, C.R., Fang, Z., Chang, S., Singh, J. 2022. Parameter study on double-row pile in the combined high retaining structure. Geotechnical and Geological Engineering, 40(10): Pp. 5233-5248.

Won, J., You, K., Jeong, S., Kim, S., 2005. Coupled effects in stability analysis of pile–slope systems. Computers and Geotechnics, 32(4): Pp. 304-315.

Xiong, C.X., Zhang, M., Chen, Y., 2022. Experimental investigation on h-type retaining structure. China Civil Engineering Journal, 55(07): Pp. 108-120.

Xu, J.S., Yang, X.L., 2018. Seismic and static stability analysis for 3D reinforced slope in nonhomogeneous and anisotropic soils. International Journal of Geomechanics, 18(7): Pp. 04018065.

Xu, W.J., Huang, X., Huang, J.D., Yang, Z.J., 2021. Structural analysis of backfill highway subgrade on the lower bearing capacity foundation using the finite element method. Advances in Civil Engineering, 2021: Pp. 1-11.

Yan, Y., Xing, Z.Q., Chen, X.L., Xie, Z., Zhang, J.W., Chen, Y., 2023. Axial compression performance of CFST columns reinforced by ultra-high-performance nano-concrete under long-term loading. Nanotechnology Reviews, 12(1): Pp. 20220537.

Zhang, T.W., Cai, Q.X., Han, L., Shu, J.S., Zhou, W., 2017. 3D stability analysis method of concave slope based on the Bishop method. International Journal of Mining Science and Technology, 27(2): Pp. 365-370.

Zhang, W.G., Goh, A.T.C., Xuan, F., 2015. A simple prediction model for wall deflection caused by braced excavation in clays. Computers and Geotechnics, 63: Pp. 67-72.

Zhao, B., Wang, Y.S., Wang, Y., Shen, T., Zhai, Y.C., 2017. Retaining mechanism and structural characteristics of h type anti-slide